Available online at www.sciencedirect.com
ScienceDirect
Carbohydrate Polymers 72 (2008) 43–51
Carbohydrate Polymers
www.elsevier.com/locate/carbpol

Impregnation of silver nanoparticles into bacterial cellulose for antimicrobial wound dressing

Thawatchai Maneerung [a], Seiichi Tokura [b], Ratana Rujiravanit [a,*]

[a] *The Petroleum and Petrochemical College, Chulalongkorn University, Bangkok 10330, Thailand*
[b] *Faculty of Engineering, Kansai University, Suita, Osaka 564-8680, Japan*

Received 4 June 2007; received in revised form 17 July 2007; accepted 18 July 2007
Available online 1 August 2007

Abstract

Bacterial cellulose was produced by *Acetobacter xylinum* (strain TISTR 975). Bacterial cellulose is an interesting material for using as a wound dressing since it provides moist environment to a wound resulting in a better wound healing. However, bacterial cellulose itself has no antimicrobial activity to prevent wound infection. To achieve antimicrobial activity, silver nanoparticles were impregnated into bacterial cellulose by immersing bacterial cellulose in silver nitrate solution. Sodium borohydride was then used to reduce the absorbed silver ion (Ag^+) inside of bacterial cellulose to the metallic silver nanoparticles (Ag^0). Silver nanoparticles displayed the *optical absorption* band around 420 nm. The red-shift and broadening of the optical absorption band was observed when the mole ratio of $NaBH_4$ to $AgNO_3$ ($NaBH_4$:$AgNO_3$) was decreased, indicating the increase in particle size and particles size distribution of silver nanoparticles that was investigated by transmission electron microscope. The formation of silver nanoparticles was also evidenced by the X-ray diffraction. The freeze-dried silver nanoparticle-impregnated bacterial cellulose exhibited strong the antimicrobial activity against *Escherichia coli* (Gram-negative) and *Staphylococcus aureus* (Gram-positive).

Keywords: *Acetobacter xylinum*; Bacterial cellulose; Silver nanoparticle; Inhibition zone; Colony forming unit; Antimicrobial activity

1. Introduction

Polymer nanocomposite containing metal nanoparticles can be prepared by several methods. One of common methods is the mechanical mixing of a polymer with metal nanoparticles, the in situ polymerization of a monomer in the presence of metal nanoparticles, or the in situ reduction of metal salts or complexes in a polymer. These polymer nanocomposites have attracted a great deal of attention, due to their unique optical, electrical, catalytic properties (Shiraishi & Toshima, 2000) and biomedical device (Schierholz, Lucas, Rump, & Pulverer, 1998). The main biomedical device that based on the polymer nanocomposite containing metal nanoparticles is the antimicrobial device that composed of polymer and metal nanoparticles, which is a mostly silver nanoparticle (Shanmugam, Viswanathan, & Varadarajan, 2006).

Silver metal and its compound have been known to have strong inhibitory and bactericidal effects as well as a broad spectrum of antimicrobial activities. Silver ions work against bacteria in a number of ways; silver ions interact with the thiol groups of enzyme and proteins that are important for the bacterial respiration and the transport of important substance across the cell membrane and within the cell (Cho, Park, Osaka, & Park, 2005; Ivan & Branka, 2004) and silver ions are bound to the bacterial cell wall and outer bacterial cell, altering the function of the bacterial cell membrane (Percival, Bowler, & Russell, 2005) thus silver metal and its compounds were the effective preventing infection of the wound (Wright, Lam, Hansen, & Burrell, 1999). Silver metal was slowly changed to silver ions under our physiological system and interact with bacterial cells, thus silver ions will not be so high enough to

* Corresponding author.
E-mail address: ratana.r@chula.ac.th (R. Rujiravanit).

0144-8617/$ - see front matter © 2007 Elsevier Ltd. All rights reserved.
doi:10.1016/j.carbpol.2007.07.025

cause normal human cells damage. Silver nanoparticles have a high specific surface area and a high fraction of surface atoms that lead to high antimicrobial activity compared to bulk silver metal (Cho et al., 2005).

The scientific basics of moist environmental healing were created by G.D. Winter in 1962. His pioneering research initiated the concept of active wound dressing, which creates and maintains the optimum conditions required for the regeneration of broken tissue. Occlusive wound dressing may come in form of form, gel, hydrogel and aerosol. They maintain the proper moisture level and constant temperature of the wound bed, accelerate healing, activate autolytic debridement of the wound, protect newly formed cells, facilitates angiogenesis and re-epithelisation, alleviate pain, and protect the wound against bacteria and contamination. Bacterial cellulose is a natural hydrogel whose properties better the hydrogel produced from synthetic polymers; for example, it displays high water content (98–99%), good sorption of liquids, high wet strength, and high chemical purity and can be safety sterilized without any change to its structure and properties (Klemm, Schumann, Udhardt, & Marsch, 2001). Being similar to human skin, bacterial cellulose can be applied as skin substitute in treating extensive burns (Czaja, Krystynowicza, Bielecki, & Malcolm Brown, 2006). Bacterial cellulose is synthesized by the acetic bacterium, *Acetobacter xylinum*. The fibrous structure of bacterial cellulose consists of a three-dimensional non-woven network of microfibrils, containing same chemical structure as plant cellulose (Czaja, Romanovicz, & Malcolm Brown, 2004), bound together by inter- and intra-fibrilar hydrogen bonding resulting in the never dried-state or hydrogel and high strength of bacterial cellulose.

Bacterial cellulose is an interesting material for using as a wound dressing since it can control wound exudates and can provide moist environment to a wound resulting in better wound healing. However, bacterial cellulose itself has no antimicrobial activity to prevent wound infection. To achieve an antimicrobial activity, in this work silver nanoparticles were impregnated into bacterial cellulose through the chemical reduction by immersing bacterial cellulose in the silver nitrate solution. Sodium borohydride was then used to reduce the absorbed silver ion (Ag^{+}) inside of bacterial cellulose to metallic silver nanoparticles (Ag^{0}).

2. Experiments

2.1. Materials

Acetobacter xylinum (strain TISTR 975), *Escherichia coli* and *Staphylococcus aureus* were purchased from Microbiological Resources Centre, Thailand Institute of Scientific and Technological Research (TISTR). Nutrient broth (Approximate formula*per liter: Beef extract 3.0 g and Peptone 5.0 g) was purchased from Difco™. Analytical grade D-glucose anhydrous was purchased from Ajax Finechem. Yeast extract powder and agar powder were bacteriological grade and purchased from HiMedia. Laboratory grade calcium carbonate and analytical grade silver nitrate were purchased from Fisher Scientific. Laboratory grade sodium borohydride was purchased from CARLO ERBA. Analytical grade sodium hydroxide anhydrate pellet and sodium chloride were purchased from Aldrich Chemical. Analytical grade glacial acetic acid was purchased from CSL Chemical. Ethanol was commercial grade and used without further purification.

2.2. Production of bacterial cellulose

2.2.1. Culture medium

Culture medium used for the fermentation of *A. xylinum* (strain TISTR 975) to produce bacterial cellulose contained D-glucose anhydrous 100.0 g, yeast extract powder 10.0 g and distilled water 1.0 L then culture medium was adjusted pH to 6.0 by 1.0% acetic acid then sterilized by autoclaving at 120 °C for 15 min, developed by Microbiological Resources Centre, Thailand Institute of Scientific and Technological Research (TISTR) (http://www.tistr.or.th/mircen/index.html).

2.2.2. Culture conditions

Pre-inoculum for all experiments was prepared by transferring a single *A. xylinum* (strain TISTR 975) colony grown on agar culture medium into a 50-mL Erlenmeyer flask filled with liquid culture medium. After 24 h of cultivation at 30 °C, bacterial cellulose pellicle produced on the surface of the culture medium was either squeezed or vigorously shaken in order to remove active cells embedded in the bacterial cellulose membrane. Ten milliliters of the cell suspension was introduced into a 500-mL Erlenmeyer flask containing 100 mL of a fresh liquid culture medium, covered by a porous paper and kept at 30 °C for 5 days.

2.2.3. Purification of bacterial cellulose

After incubation, bacterial cellulose pellicles produced on the surface of each liquid culture medium were harvested and purified by boiling them in 1.0% NaOH for 2 h (two times), treated with 1.5% acetic acid for 30 min and finally thoroughly washed in tap water until bacterial cellulose pellicles became neutral and then immersed in the distilled water prior to use.

2.3. Impregnation of silver nanoparticles into bacterial cellulose

Silver nanoparticles were impregnated into bacterial cellulose fiber by immersing bacterial cellulose pellicles in 0.001 M of the aqueous $AgNO_3$ for 1 h, followed by rinsing with ethanol for ca. 30 s. After then the silver ion-saturated bacterial cellulose pellicles were reduced in 0.001, 0.01 and 0.1 M of the aqueous $NaBH_4$ for 10 min and rinsed with a large amount of ultra-pure water for 10 min to remove the excess chemical, the obtained samples were frozen at −40 °C and dried in a vacuum at −52 °C.

2.4. Characterization

The morphology of bacterial cellulose was observed by using JEOL JSM-5200 scanning electron microscope operating at 15 kV at a magnification of 10,000×. The formation of silver nanoparticles was identified by the XRD (Rigaku). Sample was scanned from $2\theta = 30°$ to $2\theta = 80°$ at a scanning rate of 5° 2θ/min. The optical absorption of freeze-dried silver nanoparticle-impregnated bacterial cellulose was measured using a Hitachi U-2010 spectrometer. Transmission electron microscopy (TEM) observations were carried out on a JEOL JEM-2000EX instrument operated at 80 kV accelerating voltage. We prepared the TEM samples on a 400 mesh copper grid coated with carbon. Histogram, mean diameter and standard deviation were obtained by sampling 200 metal nanoparticles in TEM images of 62,000 magnifications, followed by analyses using SPSS14 program.

2.5. Release of silver ions

Freeze-dried silver nanoparticle-impregnated bacterial cellulose was cut into a disc shape with 1.5 cm of diameter, and then eight pieces of sample were immersed in 50 mL of the deionized water 1 day at 37 °C. The next day they were removed, blotted free of excess fluid, and transferred to a fresh 50 mL of the deionized water. The process was continued for 6 days. The suspending fluids from days 1, 2, 3, 4, 5 and 6 were then analyzed for silver ion by atomic absorption spectrophotometer (AAS).

2.6. Swelling

Freeze-dried silver nanoparticle-impregnated bacterial cellulose, dried to constant weight was cut into a disc shape with 1.5 cm diameter and immersed in the deionized water for the certain time at room temperature. Swelling was calculated as follows:

$$\text{Swelling} = (G_{s,t} - G_i)/G_i$$

where G_i is the initial weight of dried sample and $G_{s,t}$ is the weight of sample in swollen state.

2.7. Antimicrobial activity studies

Antimicrobial activities of freeze-dried silver nanoparticle-impregnated bacterial cellulose have been investigated against *E. coli* as the model Gram-negative bacteria and *S. aureus* as the model Gram-positive bacteria. The antimicrobial activities of freeze-dried silver nanoparticle-impregnated bacterial cellulose were carried out by two methods.

2.7.1. The disc diffusion method

This method was performed in Luria–Bertani (LB) medium solid agar Petri dish. The freeze-dried silver nanoparticle-impregnated bacterial cellulose was cut into a disc shape with 1.5 cm diameter, sterilized by autoclaving 15 min at 120 °C, and was placed on *E. coli*-cultured agar plate and *S. aureus*-cultured agar plate which were then incubated for 24 h at 37 °C and inhibition zone was monitored.

2.7.2. The colony forming count method

Freeze-dried silver nanoparticle-impregnated bacterial cellulose was cut into a disc shape with 1.5 cm diameter. Before inoculation of the bacteria, the pieces of sample were sterilized by autoclaving at 120 °C for 15 min. The experimental design is shown in Fig. 1. Sample was divided into two groups; each group consists of eight pieces. The first group was seeded with 1 mL sterile nutrient broth as sterility control. The second group was seeded with fresh *E. coli* or *S. aureus* culture at a concentration of 10^5 colony forming units per mL (cfu/mL), then incubated in shaking incubator at 37 °C for 24 h. After incubation, 50 mL saline was added to each of groups and then all tubes were vortexed. The 50 μL of bacterial suspension was drawn from each of tube, spread on a nutrient agar plate and incubated at 37 °C for 48 h for colony forming counts. The same procedure was performed on pure bacterial cellulose. The percentage reduction in bacterial count was calculated by the formula (Li, Leung, Yao, Song, & Newton, 2006):

$$\frac{(\text{Viable count at 0 h} - \text{Viable count at 24 h})}{\text{Viable count at 0 h}} \times 100\%$$

3. Results and discussion

3.1. Morphology of bacterial cellulose

The porous structure of the freeze-dried bacterial cellulose with three-dimensional non-woven structures of nanofibrils (50–100 nm) which are highly uniaxially oriented (see Fig. 2a) is observed on the surface of bacterial cellulose membrane. Whereas the multilayer of bacterial cellulose membranes linked together with the nanofibrils is observed in the cross-sectional morphology of bacterial cellulose (see Fig. 2b) due to in the process of bacterial cellulose pellicle

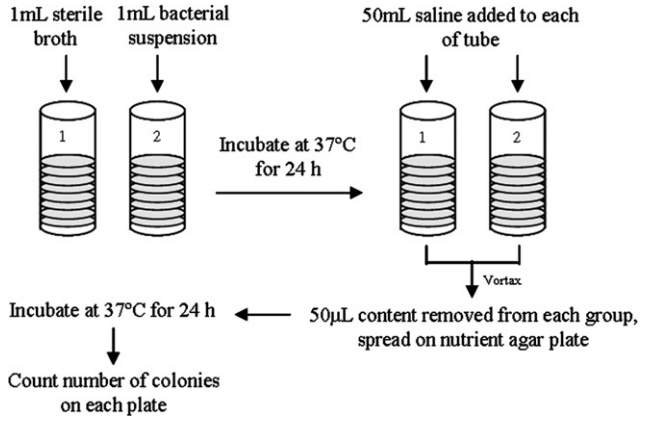

Fig. 1. Flow chart showing the experimental procedure of the colony forming count method.

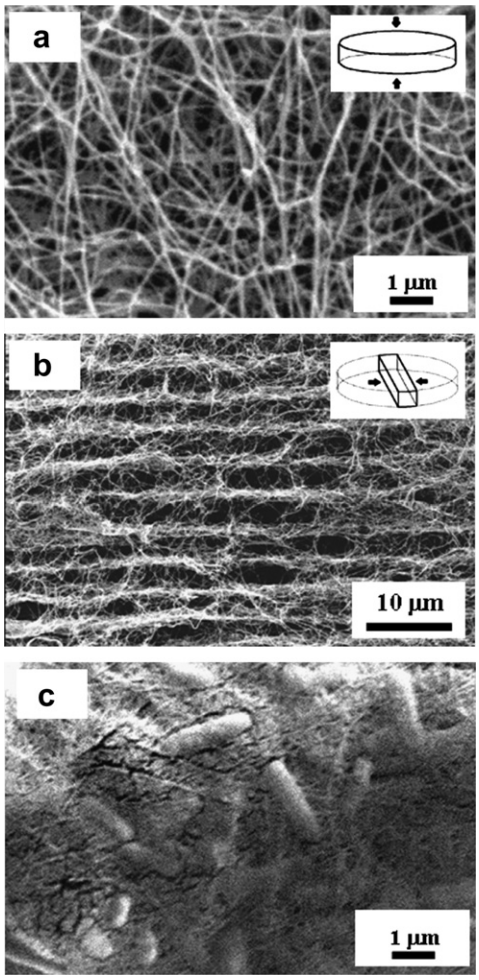

Fig. 2. SEM image of (a) surface morphology of NaOH-treated bacterial cellulose (b) cross-sectional morphology of NaOH-treated bacterial cellulose and (c) native bacterial cellulose.

growth, bacteria generate cellulose only in the vicinity of culture surface. As long as the system is kept unshaken, bacterial cellulose pellicle is suspended by the cohesion to the interior wall of flask and slides steadily downwards as it thickens (Iguchi, Yamanaka, & Budhiono, 2000). These unique nano-morphology result in a large surface area that can hold a large amount of water (up to 200 times of its dry mass) and at the same time displays great elasticity, high wet strength, and conformability (Czaja et al., 2006). In addition, the figures show the effect of NaOH treatment on the native pellicle, revealing its topological and porous structure. Intact bacteria and debris were not found in the membrane after treatment. In contrast, intact bacteria, debris and no fibrillar structure were found in the SEM image of the native bacterial cellulose (see Fig. 2c).

3.2. Impregnation of silver nanoparticles in bacterial cellulose

Structure of bacterial cellulose is three-dimensional non-woven networks and consists of large amount of pores. Thus, when bacterial cellulose was immersed in the aqueous $AgNO_3$, silver ions were readily penetrated into bacterial cellulose though their pores. The absorbed Ag^+ were bound to bacterial cellulose microfibrils probably via electrostatic interactions, because the electron-rich oxygen atoms of polar hydroxyl and ether groups of bacterial cellulose are expected to interact with electropositive transition metal cations (He, Kunitake, & Nakao, 2003). Rinsing by ethanol effectively removed those Ag^+ that were not bound to bacterial cellulose. However, it should be noted that during rinsing process, there is a little precipitate occurred, since ethanol rinsing was very slowly and carefully. And it was no turbidity observation due to the precipitation of silver nitrate by ethanol. After reduction in aqueous $NaBH_4$, silver ions were reduced to form silver nanoparticles. The original colorless bacterial cellulose was turned to yellow. Finally, the freeze-dried silver nanoparticle-impregnated bacterial cellulose was dried by the freeze-drying method to maintain the original structure of bacterial cellulose (Klemm et al., 2001) and to lock up the content of silver nanoparticles until the dressing was re-hydrated by moisture or wound exudates.

The X-ray diffraction (XRD) was used to examine the crystal structure of metal nanoparticles that used to confirm the formation of silver nanoparticles. The XRD pattern of freeze-dried silver nanoparticle-impregnated bacterial cellulose (see Fig. 3) shows characteristic four peaks at 2θ values of 38.1°, 44.3°, 64.4° and 78.0° corresponding to (111), (200), (220) and (311) planes of the face centered cubic (fcc) structure of the metallic silver nanoparticles (Jiang, Wang, Chen, Yu, & Wang, 2005; Zhang et al., 2006) that were impregnated inside of bacterial cellulose.

The color of freeze-dried silver nanoparticle-impregnated bacterial cellulose gradually changed from a brown yellow to a bright yellow with increasing molar ratio of $NaBH_4$ to $AgNO_3$ from 1:1 to 10:1 to 100:1. Fig. 4 shows the optical absorption spectra of freeze-dried silver nano-

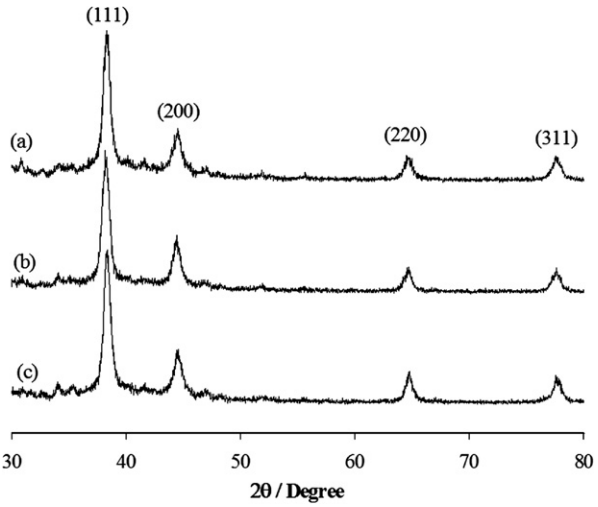

Fig. 3. XRD pattern of freeze-dried silver nanoparticle-impregnated bacterial cellulose was prepared from the $NaBH_4$:$AgNO_3$ molar ratio of (a) 1:1, (b) 10:1 and (c) 100:1.

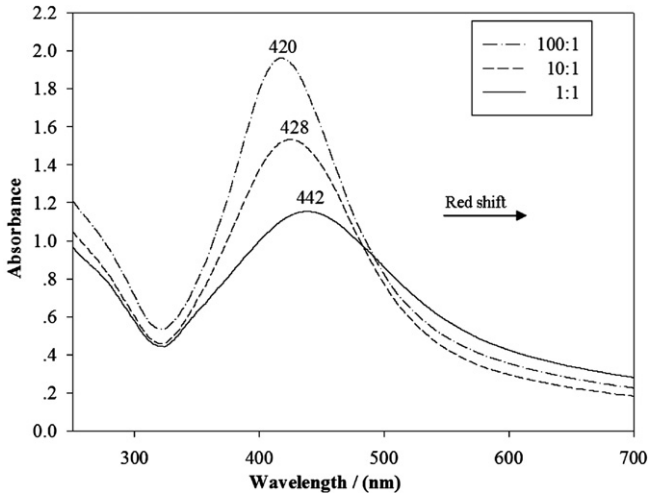

Fig. 4. Absorption spectra of freeze-dried silver nanoparticle-impregnated bacterial cellulose prepared from the $NaBH_4$:$AgNO_3$ molar ratio of 1:1, 10:1 and 100:1.

particle-impregnated bacterial cellulose, typical absorption of metallic silver nanoparticles. This is due to the surface plasmon resonance (SPR) of conducting electron (or free electron) on the surface of silver nanoparticles (Kim & Kang, 2004). Moreover, freeze-dried silver nanoparticle-impregnated bacterial cellulose was a bright yellow color, due to the intense band around the excitation of SPR (Mingwei, Guodong, Guanjun, Zhiyu, & Minquan, 2006; Temgire & Joshi, 2004). At the $NaBH_4$:$AgNO_3$ molar ratio of 100:1, a narrow absorption band is located at 420 nm. No absorption was observed at wavelengths longer than 500 nm. This implied that the small silver nanoparticles with the narrow size distribution were formed. The absorption band underwent a red-shift to 428 nm and was slightly broadened at the $NaBH_4$:$AgNO_3$ molar ratio of 10:1. The absorption band also underwent a red-shift to 442 nm and become much broadened at the $NaBH_4$:$AgNO_3$ molar ratio of 1:1. The red-shift and broadening of absorption band are possible to show the increase in a particle size and size distribution (Sönnichsen, Franzl, Wilk, Plessen, & Feldmann, 2002). This implied that the larger silver nanoparticles and the wide size distribution were probably formed when the $NaBH_4$:$AgNO_3$ molar ratio was decreased, which resulted from the excess amount of silver ions aggregated together. In contrast with the small silver nanoparticles and the narrow size distribution are formed when the $NaBH_4$:$AgNO_3$ molar ratio was increased. This is probably due to the amount of free electron generated from $NaBH_4$ is high enough to prevent the aggregation of silver.

These conclusions are confirmed by TEM observations. As shown in Fig. 5a and b, irregular shape of silver nanoparticles with the large size and the wide size distribution were obtained at the $NaBH_4$:$AgNO_3$ molar ratio of 1:1. Their mean diameter (d) and standard deviation (σ) were estimated to be 11.34 and 6.31 nm, respectively. When the $NaBH_4$:$AgNO_3$ molar ratio was increased from 1:1 to 10:1, the particle size decreased ($d = 6.48$ nm) and the size distribution become small ($\sigma = 2.68$ nm) as shown in Fig. 5c and d. The well dispersed and regular spherical silver nanoparticles were obtained at the $NaBH_4$:$AgNO_3$ molar ratio of 100:1. The particle size is much smaller ($d = 5.47$ nm) and the size distribution become rather narrow ($\sigma = 2.20$ nm) as shown in Fig. 5e and f. Therefore, the size and size distribution of silver nanoparticles can be controlled by adjusting the molar ratio of $NaBH_4$ to $AgNO_3$.

Moreover, the $NaBH_4$:$AgNO_3$ molar ratio influenced the depth of silver nanoparticles inside of bacterial cellulose which resulted from the cation concentration gradient between the absorbed Ag^+ inside bacterial cellulose and the Na^+ of the aqueous $NaBH_4$ outside bacterial cellulose during the chemical reduction of silver nanoparticles. At the $NaBH_4$:$AgNO_3$ molar ratio of 1:1, the concentration of the absorbed Ag^+ inside bacterial cellulose was equal to that of the Na^+ outside bacterial cellulose. When the Ag^+ at the surface of bacterial cellulose were reduced to form the silver nanoparticles, the cation concentration gradient was occurred and the some deeper Ag^+ penetrated to the surface and formed nanoparticles. Thus, the silver nanoparticles were formed only at the surface of bacterial cellulose and there are some absorbed Ag^+ inside bacterial cellulose pellicle as shown in Fig. 6a. At the higher $NaBH_4$:$AgNO_3$ molar ratios of 1:1 (10:1 and 100:1), silver nanoparticles which formed inside bacterial cellulose were deeper, respectively, as shown in Fig. 6b and c. Because the concentration of absorbed Ag^+ inside bacterial cellulose is much lower than concentration of Na^+ of the aqueous $NaBH_4$ thus the cation concentration gradient occurred, then Na^+ in the aqueous $NaBH_4$ penetrate into bacterial cellulose pellicles, not Ag^+ penetrate out. After that Ag^+ were reduced and formed nanoparticles inside of bacterial cellulose pellicle. On the contrary, at lower $NaBH_4$:$AgNO_3$ molar ratio of 1:1 (1:100), the concentration of absorbed Ag^+ inside bacterial cellulose pellicle is much more than the concentration of Na^+ in the aqueous $NaBH_4$ thus the cation concentration gradient occurred, then absorbed Ag^+ inside bacterial cellulose pellicle penetrate out and form nanoparticles in the solution, not bacterial cellulose pellicle, that can be observed by the color change of a clear solution of aqueous $NaBH_4$ to a yellow solution (see Fig. 6d). These conclusions were confirmed by the energy dispersive X-ray (EDX) analysis. The composition of sodium (Na) and other elements in the freeze-dried silver nanoparticle-impregnated bacterial cellulose prepared from each of the $NaBH_4$:$AgNO_3$ molar ratio were concluded in Table 1. The composition of Na in the samples was increased by increasing of the $NaBH_4$:$AgNO_3$ molar ratio, whereas boron (B), which is also the main component in the aqueous $NaBH_4$ and can cause the human tissue damage, was not found in these samples. These results implied that after the chemical reduction of silver ions in $NaBH_4$ and washing with large amount of pure water for 10 min, only Na was trapped inside of bacterial cellulose.

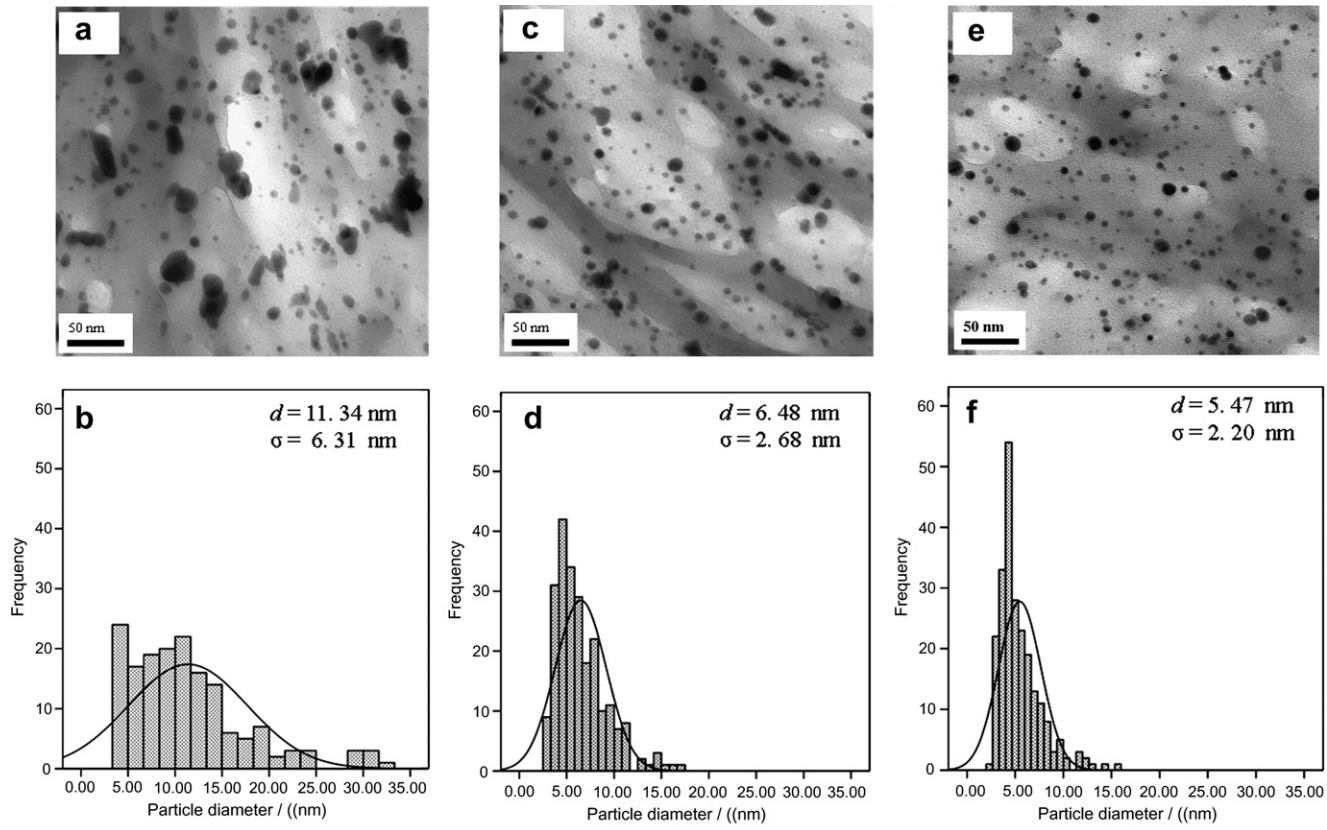

Fig. 5. TEM images and histograms of freeze-dried silver nanoparticle-impregnated bacterial cellulose prepared from the $NaBH_4$:$AgNO_3$ molar ratio of 1:1 (a and b), 10:1 (c and d) and 100:1 (e and f).

3.3. Release of silver ions

Fig. 7 shows silver ion releasing behavior of the freeze-dried silver nanoparticle-impregnated bacterial cellulose. The silver ions were released rapidly from the freeze-dried silver nanoparticle-impregnated bacterial cellulose that was prepared from the $NaBH_4$:$AgNO_3$ molar ratio of 1:1 that is due to the silver nanoparticles was impregnated only at the surface of bacterial cellulose. When the $NaBH_4$:$AgNO_3$ molar ratio was increased from 1:1 to 10:1 to 100:1, the impregnated silver nanoparticles were deeper, thus the silver ions were released gradually.

3.4. Swelling

Fig. 8 shows high swelling ability of freeze-dried silver nanoparticle-impregnated bacterial cellulose, 62.25 of swelling ratio after immersing in the deionized water for 4 h. This is due to both chemical and physical structure; for chemical structure, bacterial cellulose is hydrophilic material that is expected to absorb molecule of water (Klemm et al., 2001); for physical structure, bacterial cellulose is three-dimensional non-woven network with large amount of pores which was maintained by freeze-drying method and this physical structure is expected to generate the capillary force within network of bacterial cellulose and suck the molecules of water (Iguchi et al., 2000). High swelling ability of silver nanoparticle-impregnated bacterial cellulose is important property for wound dressing that used to control wound exudates and keep moist environment on the wound.

3.5. Antimicrobial activity studies

3.5.1. The disc diffusion method

The antibacterial activity of freeze-dried silver nanoparticle-impregnated bacterial cellulose for *E. coli* and *S. aureus* was measured by the disc diffusion method. It was found that the freeze-dried silver nanoparticle-impregnated bacterial cellulose exhibit an inhibition zone. The growth inhibition ring of *E. coli* and *S. aureus* was 2 and 3.5 mm, respectively. No inhibition zone was observed with the pure bacterial cellulose as control (see Fig. 9a and b). This clearly demonstrates that the antimicrobial activity is only due to silver nanoparticles impregnated inside bacterial cellulose and not due to individual bacterial cellulose.

3.5.2. The colony forming count method

The freeze-dried silver nanoparticle-impregnated bacterial cellulose was tested with *E. coli* and *S. aureus*, no bacterial growth was obtained from the sterility control. The viable counts recovered from the freeze-dried silver nanoparticle-impregnated bacterial cellulose before and after incubation are shown in Table 2. After 48 h of incubation,

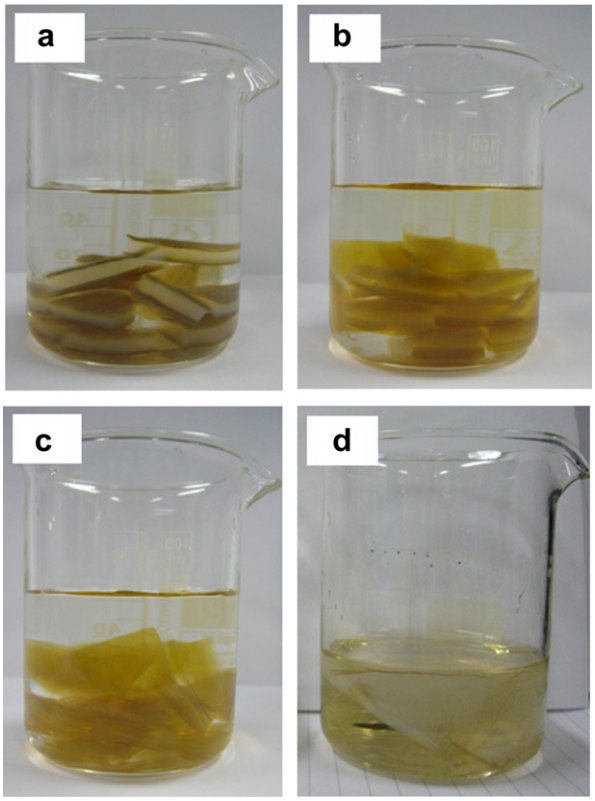

Fig. 6. The depth of silver nanoparticles impregnated into bacterial cellulose prepared from the $NaBH_4$:$AgNO_3$ molar ratio of (a) 1:1, (b) 10:1, (c) 100:1 and (d) 1:100.

Table 1
The composition of element in the freeze-dried silver nanoparticle-impregnated bacterial cellulose

$NaBH_4$:$AgNO_3$ molar ratio	% Element						
	C	O	Na	B	Ag	Au	Total
1:1	51.18	25.50	0.02	0.00	2.91	20.39	100.00
10:1	51.85	26.13	0.29	0.00	2.94	18.78	100.00
100:1	43.52	30.38	2.51	0.00	3.35	20.24	100.00

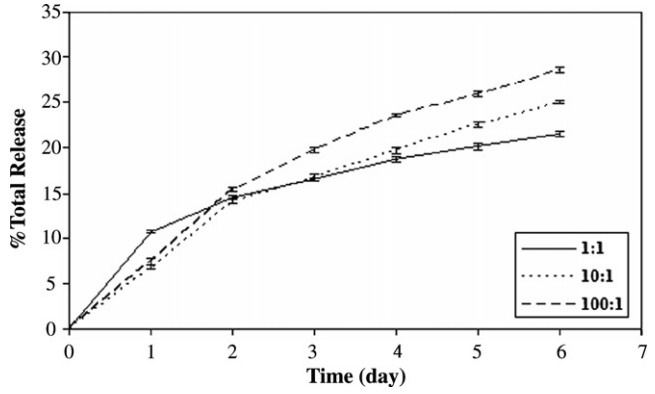

Fig. 7. Silver ion releasing behavior of the freeze-dried silver nanoparticle-impregnated bacterial cellulose prepared from the $NaBH_4$:$AgNO_3$ molar ratio of 1:1, 10:1 and 100:1.

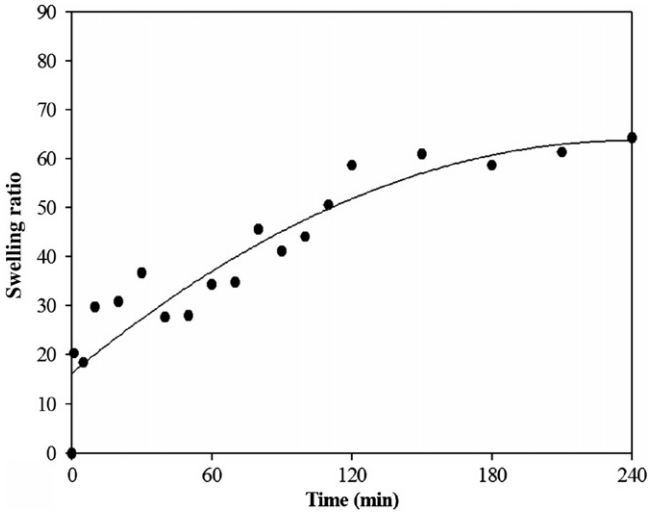

Fig. 8. Swelling ability of freeze-dried silver nanoparticle-impregnated bacterial cellulose.

there was a 99.7% and 99.9% reduction in viable *E. coli* and *S. aureus* on the freeze-dried silver nanoparticle-impregnated bacterial cellulose, respectively. For the pure bacterial cellulose, there was no reduction in viable counts; on the contrary, there was a 34.6% and 40.7% increase in the viable counts of *E. coli* and *S. aureus*, respectively. This clearly demonstrates that freeze-dried silver nanoparticle-impregnated bacterial cellulose had good antimicrobial activity for both *E. coli* (Gram-negative) and *S. aureus* (Gram-positive). The antibacterial activity against *E. coli* is lower than that against *S. aureus*, probably due to the difference in cell walls between Gram-positive and Gram-negative bacteria. The cell wall of the Gram-negative consists of lipids, proteins and lipopolysaccharides (LPS) that provide effective protection against biocides whereas that of the Gram-positive does not consists of LPS (Feng et al., 2000).

4. Conclusion

To summarize, we succeeded in the chemical reduction of silver nanoparticles in the three-dimensional non-woven networks of bacterial cellulose nanofibrils. The size and size distribution are controllable by adjusting the molar ratio of $NaBH_4$:$AgNO_3$. Under the optimized conditions, well dispersed and regular spherical silver nanoparticles were obtained. The unique structure and the high oxygen (ether and hydroxyl) density of bacterial cellulose fibers constitute an effective nanoreactor for in situ synthesis of silver nanoparticles. These properties are essential for introduction of silver ion and reduction into bacterial cellulose fibers and removal of the excess chemical from bacterial cellulose fibers. The ether oxygen and the hydroxyl group not only anchor silver ions tightly onto bacterial cellulose fibers via ion–dipole interactions, but also stabilize silver nanoparticles by strong interaction with their surface metal atoms. The preparative procedure is surprisingly simple.

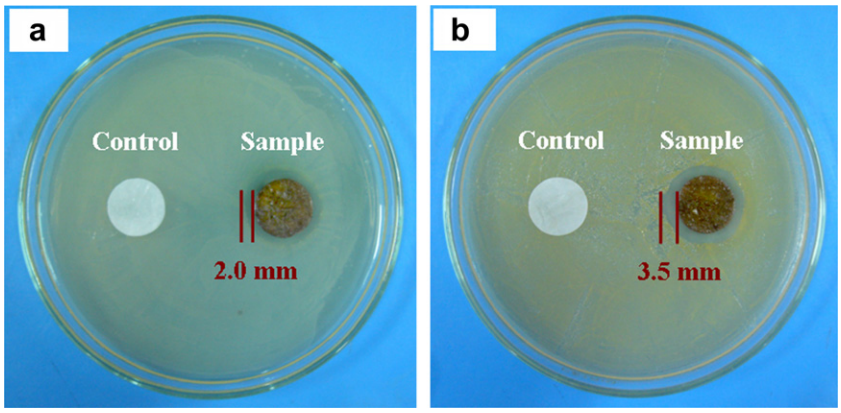

Fig. 9. Antimicrobial activity of freeze-dried silver nanoparticle-impregnated bacterial cellulose prepared from the $NaBH_4$:$AgNO_3$ molar ratio of 100:1 against (a) *Escherichia coli* and (b) *Staphylococcus aureus*.

Table 2
Colony forming unit counts (cfu/mL) at 0-h and 24-h contact time intervals with the freeze-dried silver nanoparticle-impregnated bacterial cellulose prepared from the $NaBH_4$:$AgNO_3$ molar ratio of 100:1 against (a) *Escherichia coli* and (b) *Staphylococcus aureus*

Contact time	*Escherichia coli*		*Staphylococcus aureus*	
	Impregnated BC	Pure BC	Impregnated BC	Pure BC
0 h	1.10×10^5	1.10×10^5	1.50×10^5	1.50×10^5
24 h	3.42×10^2	1.48×10^5	1.40×10^2	2.20×10^5
% of reduction/increase	99.7% reduction	34.6% increase	99.9% reduction	40.7% increase

It can provide a facile approach toward manufacturing of metallic nanocomposites, antimicrobial materials, low-temperature catalysts and other useful materials.

The freeze-dried silver nanoparticle-impregnated bacterial cellulose exhibited a strong antimicrobial activity against both *S. aureus* (Gram-positive bacteria) and *E. coli* (Gram-negative bacteria), which are general bacteria that found on the contaminated wound. A recent study showed that impregnation, instead of coating the wound dressing with silver nanoparticle or nanocrystal improved the antimicrobial activity of the wound dressing and lowered possibility of the normal human tissue damage. This is probably due to the slow and continual release of silver nanoparticles and then was slowly changed to silver ions under our physiological system and interact with bacterial cells, thus silver ions will not be so high enough to cause the normal human cells damage and can prolonged the antimicrobial effect.

Acknowledgements

Financial support from the Petroleum and Petrochemical College, Chulalongkorn University and the National Excellence Center for Petroleum, Petrochemicals and Advanced Materials, Thailand is greatly acknowledged.

References

Cho, K. H., Park, J. E., Osaka, T., & Park, S. G. (2005). The study of antimicrobial activity and preservative effects of nanosilver ingredient. *Electrochimica Acta, 51*, 956–960.

Czaja, W., Romanovicz, D., & Malcolm Brown, R. Jr., (2004). Structural investigations of microbial cellulose produced in stationary and agitated culture. *Cellulose, 11*, 403–411.

Czaja, W., Krystynowicza, A., Bielecki, S., & Malcolm Brown, R. Jr., (2006). Microbial cellulose – The natural power to heal wounds. *Biomaterials, 27*, 145–151.

Feng, Q. L., Wu, J., Chen, G. Q., Cui, F. Z., Kim, T. N., & Kim, J. O. (2000). A mechanistic study of the antibacterial effect of silver ions on *Escherichia coli* and *Staphylococcus aureus*. *Journal of Biomedical Material Research, 52*(4), 662–668.

He, J., Kunitake, T., & Nakao, A. (2003). Facile in situ synthesis of noble metal nanoparticles in porous cellulose fibers. *Chemistry of Materials, 15*, 4401–4406.

http://www.tistr.or.th/mircen/index.html.

Iguchi, M., Yamanaka, S., & Budhiono, A. (2000). Bacterial cellulose – A masterpiece of nature's arts. *Journal of Materials Science, 35*(2), 261–270.

Ivan, S., & Branka, S. S. (2004). Silver nanoparticles as antimicrobial agent: A case study on *E. coli* as a model for Gram-negative bacteria. *Journal of Colloid and Interface Science, 275*, 177–182.

Jiang, G. H., Wang, L., Chen, T., Yu, H. J., & Wang, J. J. (2005). Preparation and characterization of dendritic silver nanoparticles. *Journal of Materials Science, 40*, 1681–1683.

Kim, Y. H., & Kang, Y. S. (2004). Synthesis and characterization of Ag nanoparticles, Ag–TiO_2 nanoparticles and Ag–TiO_2–chitosan complex and their application to antibiosis and deodorization. *Materials Research Society, 820*, 161–166.

Klemm, D., Schumann, D., Udhardt, U., & Marsch, S. (2001). Bacterial synthesized cellulose-artificial blood vessels for microsurgery. *Progress in Polymer Science, 26*(9), 1561–1603.

Li, Y., Leung, P., Yao, L., Song, Q. W., & Newton, E. (2006). Antimicrobial effect of surgical masks coated with nanoparticles. *Journal of Hospital Infection, 62*, 58–63.

Mingwei, Z., Guodong, Q., Guanjun, D., Zhiyu, W., & Minquan, W. (2006). Plasma resonance of silver nanoparticles deposited on the

surface of submicron silica spheres. *Materials Chemistry and Physics, 96*, 489–493.

Percival, S. L., Bowler, P. G., & Russell, D. (2005). Bacterial resistance to silver in wound care. *Journal of Hospital Infection, 60*, 1–7.

Schierholz, J. M., Lucas, L. J., Rump, A., & Pulverer, G. (1998). Efficacy of silver-coated medical devices. *Journal of Hospital Infection, 40*, 257–262.

Shanmugam, S., Viswanathan, B., & Varadarajan, T. K. (2006). A novel single step chemical route for noble metal nanoparticles embedded organic–inorganic composite films. *Materials Chemistry and Physics, 95*, 51–55.

Shiraishi, Y., & Toshima, N. (2000). Oxidation of ethylene catalyzed by colloidal dispersions of poly(sodium acrylate)-protected silver nanoclusters. *Colloids and Surfaces A: Physicochemical and Engineering Aspects, 169*, 59–66.

Sönnichsen, C., Franzl, T., Wilk, T., Plessen, G. V., & Feldmann, J. (2002). Plasmon resonances in large noble-metal clusters. *New Journal of Physics, 4*, 93.1–93.8.

Temgire, M. K., & Joshi, S. S. (2004). Optical and structural studies of silver nanoparticles. *Radiation Physics and Chemistry, 71*, 1039–1044.

Wright, J. B., Lam, K., Hansen, D., & Burrell, R. E. (1999). Efficacy of topical silver against fungal burn wound pathogens. *American Journal of Infection Control, 27*(4), 344–350.

Zhang, J., Liu, K., Dai, Z., Feng, Y., Bao, J., & Mo, X. (2006). Formation of novel assembled silver nanostructures from polyglycol solution. *Materials Chemistry and Physics, 100*, 106–112.